Journal of Nuclear Medicine, published on July 17, 2020 as doi:10.2967/jnumed.120.249748

Brief Communication, JNM

Oncology-inspired treatment options for COVID-19

Nagavarakishore Pillarsetty,[1] Lukas M. Carter,[1] Jason S. Lewis,[1,2] Thomas Reiner[1,3]*

[1] Department of Radiology, [2] Molecular Pharmacology Program and [3] Chemical Biology Program, Memorial Sloan Kettering Cancer Center, New York, NY, USA.

First author:
Nagavarakishore Pillarsetty, PhD
Memorial Sloan Kettering Cancer Center
1275 York Avenue, New York, 10065, NY, USA
Phone: 646 888 2221; Email: Pillarsn@mskcc.org; Fax:646 422 0408

Correspondence to:
Thomas Reiner, PhD
Memorial Sloan Kettering Cancer Center
1275 York Avenue, New York, 10065, NY, USA
Phone: 646 888 3461; Email: Reinert@mskcc.org; Fax:646 422 0408

Rationale: CR3022 is a human antibody which binds to the SARS-CoV-2 virus. Here, we explore the use of CR3022 as a molecularly targeted radiotherapeutic.

Methods: CR3022 was labeled with Iodine-131 using the Iodogen-method and purified, yielding [^{131}I]I-CR3022. Using a magnetic bead assay and a recombinant SARS-CoV-2 spike protein fragment, we tested binding of [^{131}I]I-CR3022 in the presence and absence of CR3022.

Results: We conjugated the antibody CR3022 with a purity > 98% and a specific activity > 292 MBq/mg. Using a bead-based assay, we confirmed that binding of [^{131}I]I-CR3022 is selective, and is significantly reduced in the presence of unlabeled antibody (3.14 ± 0.14 specific uptake and 0.10 ± 0.01 specific uptake, respectively; $P < 0.0001$).

Conclusion: Our results confirm the potential of CR3022 as a molecularly targeted probe for SARS-CoV-2. A labeled version of CR3022 could potentially be used for Auger radiotherapy or non-invasive imaging.

Keywords: Auger, Radiotherapy, COVID-19, SARS-CoV-2, CR3022.
Running title: Molecular targeting of SARS-CoV-2

INTRODUCTION

Radiotherapy, the treatment of disease with ionizing radiation, plays a significant role in the treatment and management of cancer. Most recently, molecularly targeted endoradiotherapeutics have received significant attention (*1*). These agents consist of a targeted vector (a small molecule, a peptide, an antibody) and a radioactive payload (an α-emitter, a β-emitter or an Auger emitter). Some of these treatments have generated impressive responses, as with [^{177}Lu]Lu-DOTATATE (Lutathera), a recently FDA-approved β-emitter with a half-life of 6.7 days that extends both progression-free and overall survival in the setting of midgut neuroendocrine tumors (*2*).

For molecularly targeted endoradiotherapeutics, a particular focus has to be placed on the kind of radioactive emitter, as different disintegration pathways produce particle emissions of varying type and profile (*3,4*). Matching the half-life and decay type to a particular application is therefore imperative and can determine success and failure.

The most recognized radioactive emissions of therapeutic relevance are α or β particles, which represent a $^{4}_{2}\mathrm{He}^{2+}$ nucleus and an electron, respectively. α-emitting radioisotopes have particle pathlengths of 50–100 μm and high linear energy transfer (*5*) rates (80 keV/μm). β-emitting radioisotopes have particle pathlengths of up to several mm in soft tissue and significantly lower linear energy transfer rates (~0.2 keV/μm). With the coronavirus disease 2019 (COVID-19) pandemic in mind, both α and β particles are therefore likely sub-optimal therapeutics, considering severe acute respiratory syndrome coronavirus 2 (SARS-CoV-2) virions' diameters (80–120 nM, (*6*)) and the associated potential for detrimental effects on surrounding tissue. However, Auger electron emitters appear to be of particular significance here. Auger electrons combine a relatively high LET (4–26 keV/μm) with extremely short nm-μm particle path lengths, concentrating their cytotoxic potential into minute volumes compared with cellular dimensions. In a rough approximation, Auger electrons with energies between 0.5 and 10 keV are sufficiently energetic to penetrate deep into the virus producing direct and indirect radiological effects (i.e. therapeutic action) when originating at the viral envelope, but are insufficiently energetic to directly damage neighboring cell nuclei.

In oncology, such characteristics led to attempts to incorporate Auger electrons into artificial nucleotides in order to treat cancers by causing complex DNA damage in tumor cells, but this approach has ultimately not been successful due to the difficulty of delivering lethal doses to a large enough fraction of tumor cells within a particular lesion (*7-9*). Recent preclinical work, using different delivery mechanisms, suggests a renewed promise and corroborates the considerable toxic effect of Auger emitters on tumor cells (*10*). In Figure 1, we illustrate the relationship between Auger/conversion electron energy and yield for ^{125}I. Examples for other prolific auger emitters (*11*) can be found in Figure 2.

^{125}I is reactor-produced and available in large quantities. At the time of writing, the McMaster nuclear reactor in Hamilton, Ontario produces the isotope predominantly for brachytherapy, allowing treatment of 70,000 patients annually.

In the past, ^{125}I was explored as an Auger-based radiotherapeutic for a genetically engineered measles virus. The virus, which expressed the sodium iodide symporter in infected cells, was sensitive to ^{125}I in vitro, where virus replication could be stopped. These results, however, did not translate to an in vivo model, suggesting sub-optimal pharmacokinetics of [^{125}I]-iodide (*12*). A selective, molecularly targeted vector such as the monoclonal antibody (mAb) CR3022 could serve as a delivery agent for ^{125}I. CR3022 binds to the SARS-CoV-2 receptor binding domain (RBD) with a K_D of 6.3 nM. The antibody is cross-reactive and conserved across several coronaviruses, making it ideal for targeting SARS-CoV-2, but potentially also related diseases (*13,14*).

Another iodine isotope, ^{131}I, is used not only as a standard-of-care treatment for certain types of thyroid cancers but also finds widespread use in scintigraphies and whole body SPECT imaging. Intuitively, a radiolabeled CR3022 could be valuable for imaging, potentially serving as a direct, spatially resolved, contemporaneous and non-invasive readout of viral load within a patient. From a drug-development perspective, a direct readout of SARS-CoV-2 viral load could represent a quick, upstream indicator of therapy success. This could be particularly interesting as a tool for clinical research, and similar approaches have been used to accelerate oncologic drug development pipelines in the past (*15*).

MATERIALS AND METHODS

General

All reagents were obtained from commercial vendors and used without any further purification. 0.9% Phosphate buffered saline (PBS), Iodogen® and dichloromethane were obtained from Thermo Fisher Scientific (Waltham, MA). Anti-SARS-CoV-2 antibody CR3022 was purchased from Creative Biolabs (Shirley, NY). Recombinant SARS-CoV-2 spike protein - S1 subunit (host cell receptor binding domain - RBD) with N-terminal histidine tag was purchased from Raybiotech (Peachtree Corners, GA, catalog # 230-01102-100). 1-micron diameter magnetic beads functionalized with Ni-NTA (Nickel-Nitrilotriacetic acid; HisPur™ Ni-NTA magnetic beads; Catalog # 88831) used for bead assay were purchased from Thermo Fisher Scientific. Iodogen® (1,3,4,6-tetrachloro-3α,6α-diphenyl-glycoluril, catalog # PI28600) coated glass reaction tubes were prepared by evaporating 50 µL of Iodogen® solution (50 µg, 1 mg/mL) in a borosilicate glass test tube (12 x 75 mm, catalog # 14-961-26). PD MiniTrap G-25 columns (GE Healthcare, catalog # 28918007) were preconditioned with 2 mL of PBS (Catalog # 10-010-023) before using for separating radioiodinated antibody from the free radioiodine.

Radiosynthesis

70 µL of PBS was added to an Iodogen (100 µg) precoated culture tube. To the resulting solution 25 µg of CR3022 mAb (25 µL, 1.0 mg/mL) was added. To the solution 9.25 MBq (250 µCi) of [^{131}I]I-NaI (in 17 µL of 0.1 N NaOH) was added to the tube and the mixture was allowed to react for 4 min at room temperature and loaded onto a PD MiniTrap G-25 column (GE Healthcare, catalog # 28918007) which was preconditioned with 2 mL of PBS. The radiolabeled antibody was purified using saline as eluant. The fraction #3 was used for the binding studies. The purity of the compound was measured using SG-ITLC paper using 10% trifuloroacetic acid in water as eluent. The specific activity of the final product was 292 MBq/mg (7.9 mCi/mg; 177.5 µCi/22.5 µg).

Magnetic bead assay

We have described the details of the bead-based assay in a previous publication (PMID: 31128476). The assay comprises of three separate arms – control with no antigen, positive control

and a blocking control and each arm analyzes samples in triplicates. The first arm serves as a control to measure non-specific binding (NSB) of the radioligand to the beads without any target antigen (SARS-CoV-2 spike protein - S1 subunit - SARS-CoV-2 –S1), the second arm assesses radioligand binding to SARS-CoV-2-S1 coated beads, and the third arm validates the specificity of radioligand binding to the cognate antigen in the presence of an excess of unlabeled ligand.

Briefly, samples were prepared by aliquoting 20 µL of the magnetic bead slurry into a 1.5 mL lo-bind microcentrifuge tube (13-698-794; Fisher Scientific). The beads were washed by adding 380 µL of PBS-BSA (PBS containing 1% bovine serum albumin) and the tubes were vortexed for 5 s followed by a brief spin in a mini-centrifuge prior to placing the tubes on a magnetic rack (12321D; DynaMag™-2; ThermoFisher Scientific) for 30–45 s to isolate the magnetic beads. The SARS-CoV-2 –S1 antigen was resuspended to achieve a concentration of a 0.1 mg/mL. The washed beads were resuspended in 390 µL of PBS-BSA and the beads in all tubes except the control arm were incubated with 1 µg (10 µL) of His-tagged or biotinylated antigen for 15 min on an Eppendorf™ Thermomixer at 300 RPM at room temperature. Subsequently, the beads were washed once with 400 µL of PBS-T before adding 1 ng of the radiolabeled antibody ([^{131}I]I-CR3022) resuspended in 1% BSA-PBS. [^{131}I]I-CR3022 was incubated with antigen coated beads for 30 min on a rotating mixer at room temperature. A large excess (5 µg) of the unlabeled cold antibody CR3022 was added a few seconds prior to adding 1 ng of the radioligand to antigen-coated beads in the blocking arm. Thereafter, the beads were isolated using a magnet, and the supernatant containing unbound radioligand was aspirated with a pipette and collected in separate tubes. To remove non-specifically-bound radioligand, the beads were washed twice with 400 µL of PBS-BSA. Finally, the beads, supernatant and washes were measured for radioactivity on a gamma counter. The relative binding fractions were determined by dividing percentage of total activity bound to magnetic beads to the total activity (beads + supernatants + wash).

RESULTS AND DISCUSSION

SARS-CoV-2 is a coronavirus which emerged in late 2019 and has resulted in an ongoing pandemic, causing cases of COVID-19 across the globe. Common symptoms include fever, cough, shortness of breath and muscle aches (*16*). SARS-CoV-2 enters host cells via the angiotensin-converting enzyme 2 receptor (ACE2), which is expressed in type II alveolar cells of the lungs, and can severely affect lung function (*17,18*).

Intuitively, many lessons learned from attempts to treat tumors with Auger emitters could be adapted for radiotherapeutically inactivating extracellularly circulating SARS-CoV-2 in patients. After all, tumor cells and SARS-CoV-2 share an important hallmark in their ability to evade patients' immune systems (*19,20*). However, while tumor cells may permanently escape the immune system (or only become tolerant over the course of the disease), pathogens like SARS-CoV-2 can be efficiently eliminated once adaptive immunity has been acquired (*21*). While it is unlikely that treatment of SARS-CoV-2, mediated by a radiotherapeutic Auger emitter, can lead to elimination of all virions, radiotherapy could be used in combination with other treatments and consequently improve outcomes (Fig. 1). Such treatment combinations could include currently tested treatments, including anti-IL-6 antibodies or remdesivir. However, radiation therapy was reported to initiate and influence the inflammatory and immune system (*22*), and care has to be taken that this does not negatively affect the likelihood of cytokine storms (*23*).

As a proof-of-concept that molecular targeting of SARS-CoV-2 is possible, we turned to CR3022, a human IgG1 antibody constructed from RNA, which was isolated from the lymphocytes of a convalescent SARS-CoV patient originating from Singapore (*24*). While CR3022 is therefore a potent binder of the SARS-CoV-2 RBD, the recognized epitope does not overlap with the ACE2 binding site (the receptor binding motif, RBM), and CR3022 consequently does not compete with ACE2 for binding to SARS-CoV-2. This is notably not a drawback for Auger radiotherapy of SARS-COV-2. Using Iodogen for iodination, a method established both in preclinical and clinical settings (*25,26*), we covalently conjugated ^{131}I to commercially available CR3022 with a purity of > 98% and a specific activity of 292 MBq/mg (Fig. 1C). We confirmed that the modified [^{131}I]I-CR3022 retained its potent binding to SARS-CoV-2 using a magnetic bead assay, testing its binding to a recombinant His-tagged SARS-CoV-2 RBD.

The specific binding of [^{131}I]I-CR3022 alone was significantly higher without pre-incubation of unlabeled CR3022, confirming both that CR3022 binds to SARS-CoV-2 and that binding is not perturbed after covalent modification with Iodine-131 (3.14 ± 0.14 and 0.10 ± 0.01 specific uptake for [^{131}I]I-CR3022 and CR3022, respectively; $P < 0.0001$; Fig. 1D). We consider this experiment a potent first step toward translating an orthogonal therapeutic approach for SARS-CoV-2, which could potentially be used as a combination or monotherapy for patients with active infection. The translational hurdles for such a drug could be lower than with traditional therapeutics or vaccines, because the pharmacokinetics (which are dictated by the antibody) are decoupled from the pharmacodynamics (dictated by the radioisotope). While both work synergistically, they can be optimized separately, similar to what has been done for [^{177}Lu]Lu-PSMA and [^{225}Ac]Ac-PSMA, two anti-cancer radiotherapeutics (*27*). Substitution of the isotope preserved the pharmacokinetic profile while simultaneously showing therapeutic efficacy in patients with acquired resistance to [^{177}Lu]Lu-PSMA.

Lastly, the integration of other, previously oncologically deployed strategies could lead to the rapid rollout of SARS-CoV-2 therapeutics as well, including the conjugation of drug-conjugates for treating affected cells, or known antigens for efficiently decloaking SARS-CoV-2 from the immune system.

CONCLUSION

Our preliminary data, in combination with the available literature, suggests further development of a radiotherapeutic CR3022, which would be merging different pharmacological approaches.

ACKNOWLEDGEMENTS

We thank the Small Animal Imaging Core, the Radiochemistry and Molecular Imaging Probes Core, and the Molecular Cytology Core at Memorial Sloan Kettering Cancer Center. This work was supported by National Institutes of Health grants R01 CA204441, R35 CA232130 and P30 CA008748. The authors thank the Tow Foundation and Memorial Sloan Kettering Cancer Center's Center for Molecular Imaging & Nanotechnology (CMINT) and the Memorial Sloan Kettering Cancer Center Imaging and Radiation Sciences Program.

KEY POINTS

Question

Can the human monoclonal antibody CR3022 be used as a specific targeted vector for shuttling activity to SARS-CoV-2 virions?

Pertinent findings

Labeling of CR3022 is possible, and binding affinity of the antibody for the SARS-CoV-2 receptor binding domain is retained.

Implications for patient care

CR3022, modified with a radiolabel, could be used for direct imaging of SARS-CoV-2, but also potentially as an Auger radiotherapeutic in patients with active infection.

DISCLOSURE

No conflicts of interest are noted.

REFERENCES

1. Jadvar H. Targeted radionuclide therapy: an evolution toward precision cancer treatment. *Am J Roentgenol.* 2017;209:277-288.

2. Strosberg J, El-Haddad G, Wolin E, et al. Phase 3 trial of 177Lu-Dotatate for midgut neuroendocrine tumors. *N Engl J Med.* 2017;376:125-135.

3. Poty S, Francesconi LC, McDevitt MR, Morris MJ, Lewis JS. α-Emitters for radiotherapy: from basic radiochemistry to clinical studies—part 2. *J Nucl Med.* 2018;59:1020-1027.

4. Blower PJ. A nuclear chocolate box: the periodic table of nuclear medicine. *Dalton Trans.* 2015;44:4819-4844.

5. O'Connor JP, Aboagye EO, Adams JE, et al. Imaging biomarker roadmap for cancer studies. *Nat Rev Clin Oncol.* 2017;14:169-186.

6. Liu C, Yang Y, Gao Y, et al. Viral architecture of SARS-CoV-2 with post-fusion spike revealed by cryo-EM. *bioRxiv.* 2020; https://www.biorxiv.org/content/10.1101/2020.03.02.972927v1 (Accessed on June 18th, 2020).

7. Hofer KG, Hughes WL. Radiotoxicity of intranuclear tritium, 125 iodine and 131 iodine. *Radiat res.* 1971;47:94-109.

8. Kassis AI. Cancer therapy with Auger electrons: are we almost there? *J Nucl Med.* 2003;44:1479-1481.

9. Bavelaar BM, Lee BQ, Gill MR, Falzone N, Vallis KA. Subcellular targeting of theranostic radionuclides. *Front Pharmacol.* 2018;9:996.

10. Pirovano G, Jannetti SA, Carter LM, et al. Targeted brain tumor radiotherapy using an Auger emitter. *Clin Cancer Res.* 2020;26:2871-2881.

11. Ku A, Facca VJ, Cai Z, Reilly RM. Auger electrons for cancer therapy–a review. *EJNMMI Radiopharm Chem.* 2019;4:1-36.

12. Dingli D, Peng K-W, Harvey ME, et al. Interaction of measles virus vectors with Auger electron emitting radioisotopes. *Biochem Biophys Res Commun.* 2005;337:22-29.

13. Tian X, Li C, Huang A, et al. Potent binding of 2019 novel coronavirus spike protein by a SARS coronavirus-specific human monoclonal antibody. *Emerg Microbes Infect.* 2020;9:382-385.

14. Yuan M, Wu NC, Zhu X, et al. A highly conserved cryptic epitope in the receptor binding domains of SARS-CoV-2 and SARS-CoV. *Science.* 2020;368:630-633.

15. Wang Y, Ayres KL, Goldman DA, et al. 18F-fluoroestradiol PET/CT measurement of estrogen receptor suppression during a phase I trial of the novel estrogen receptor-targeted therapeutic GDC-0810: using an imaging biomarker to guide drug dosage in subsequent trials. *Clin Cancer Res.* 2017;23:3053-3060.

16. Chen N, Zhou M, Dong X, et al. Epidemiological and clinical characteristics of 99 cases of 2019 novel coronavirus pneumonia in Wuhan, China: a descriptive study. *Lancet.* 2020;395:507-513.

17. Hoffmann M, Kleine-Weber H, Schroeder S, et al. SARS-CoV-2 cell entry depends on ACE2 and TMPRSS2 and is blocked by a clinically proven protease inhibitor. *Cell.* 2020;181:271-280.

18. Walls AC, Park Y-J, Tortorici MA, Wall A, McGuire AT, Veesler D. Structure, function, and antigenicity of the SARS-CoV-2 spike glycoprotein. *Cell.* 2020;181:281-292.

19. Willimsky G, Blankenstein T. Sporadic immunogenic tumours avoid destruction by inducing T-cell tolerance. *Nature.* 2005;437:141-146.

20. Vesely MD, Kershaw MH, Schreiber RD, Smyth MJ. Natural innate and adaptive immunity to cancer. *Annu Rev Immunol.* 2011;29:235-271.

21. Pancer Z, Cooper MD. The evolution of adaptive immunity. *Annu Rev Immunol.* 2006;24:497-518.

22. McKelvey KJ, Hudson AL, Back M, Eade T, Diakos CI. Radiation, inflammation and the immune response in cancer. *Mamm genome.* 2018;29:843-865.

23. Ye Q, Wang B, Mao J. The pathogenesis and treatment of the 'cytokine storm' in COVID-19. *J Infect.* 2020;80:607-613.

24. Ter Meulen J, Van Den Brink EN, Poon LL, et al. Human monoclonal antibody combination against SARS coronavirus: synergy and coverage of escape mutants. *PLoS Med.* 2006;3:e237.

25. Cheung N-KV, Landmeier B, Neely J, et al. Complete tumor ablation with iodine 131-radiolabeled disialoganglioside GD2-specific monoclonal antibody against human neuroblastoma xenografted in nude mice. *J Natl Cancer Inst.* 1986;77:739-745.

26. Kramer K, Humm JL, Souweidane MM, et al. Phase I study of targeted radioimmunotherapy for leptomeningeal cancers using intra-Ommaya 131-I-3F8. *J Clin Oncol.* 2007;25:5465-5470.

27. Kratochwil C, Bruchertseifer F, Giesel FL, et al. 225Ac-PSMA-617 for PSMA-targeted α-radiation therapy of metastatic castration-resistant prostate cancer. *J Nucl Med.* 2016;57:1941-1944.

28. Eckerman K, Endo A. ICRP Publication 107. Nuclear decay data for dosimetric calculations. *Ann ICRP.* 2008;38:7-96.

FIGURES

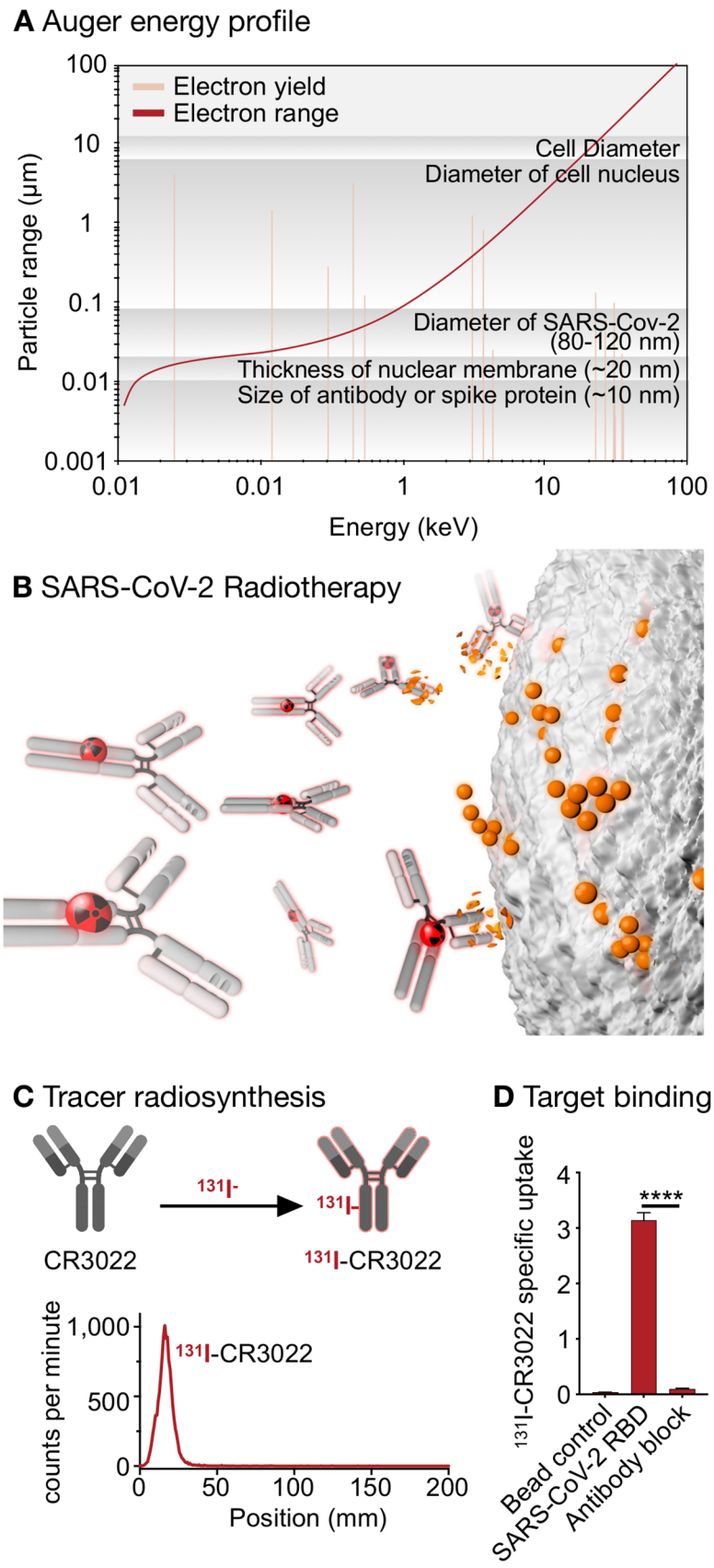

Figure 1. A new trick for an old dog. (A) Destruction of tumor cells with targeted radioactive isotopes is an important part of standard of care oncology. [^{125}I]Iodine has an energy profile which would allow deposition of energy within the radius of a SARS-CoV-2 virion. (B) Decay events damage sensitive DNA within a tumor cell nucleus, causing catastrophic single- and double strand breaks. Clinical use of Antibody-delivered Auger emitters could open a window for the targeted destruction of extracellular COVID-19 virions, decreasing the viral load during active infection and potentially easing the disease burden for a patient. (C) Labeling of CR3022 with [^{131}I]Iodine and (D) confirmation of specific binding the the SARS-COV-2 spike protein - S1 subunit (**** = P < 0.0001, unpaired Student's t test).

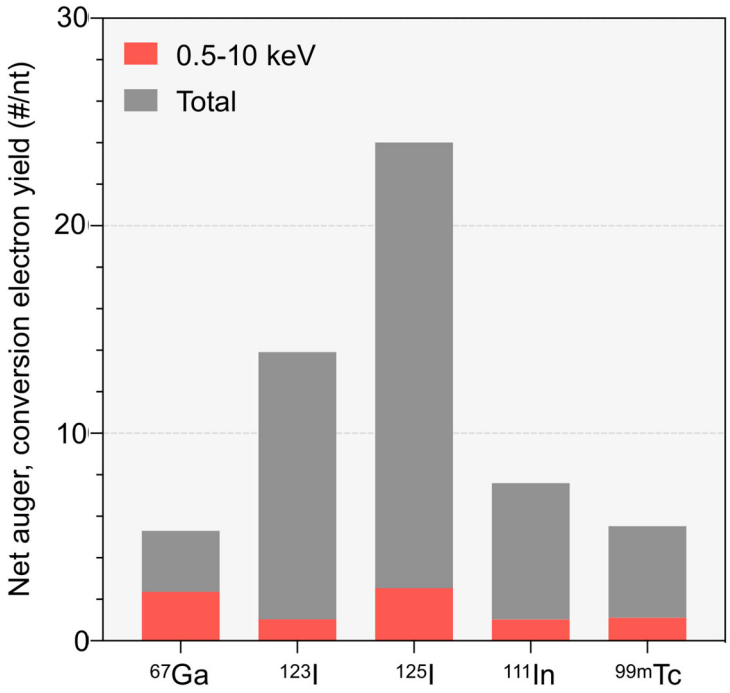

Figure 2. Net yields of monoenergetic electrons (Auger, conversion electrons) per nuclear transformation for ^{67}Ga, ^{123}I, ^{125}I, ^{111}In, and ^{99m}Tc. The red bars represent the contribution to the total yield, of electrons within the 0.5 – 10 keV energy range. Yields were obtained from ICRP Publication 107 (*28*).